Bulgarian Chemical Communications, Volume 40, Number 3 (pp. 360–366) 2008

Synthesis and characterization of novel nanostructured carbon for supercapacitors on the basis of biomaterials

M. Mladenov[1]*, P. Zlatilova[1], R. Raicheff[1], S. Vassilev[1], N. Petrov[2], K. Belov[3], V. Trenev[3], D. Kovacheva[4]

[1] *Institute of Electrochemistry and Energy Systems, Bulgarian Academy of Sciences, 1113 Sofia, Bulgaria*
[2] *Institute of Organic Chemistry, Bulgarian Academy of Sciences, 1113 Sofia, Bulgaria*
[3] *Central Laboratory of Mechatronics and Instrumentation, Bulgarian Academy of Sciences, 1113 Sofia, Bulgaria*
[4] *Institute of General and Inorganic Chemistry, Bulgarian Academy of Sciences, 1113 Sofia, Bulgaria*

Received June 23, 2008, Revised July 2, 2008

Nanoporous carbon is synthesized by steam activation of a carbonized mixture of furfural and pyrolyzed tar from apricot stones and evaluated in nonaqueous supercapacitor constructed as a two-electrode cell. Two types of supercapacitors with different non-aqueous electrolytes with working voltage range 1.25–2.5 V were developed. The initial specific capacitance of the cell with $LiBF_4$–PC electrolyte is 16.2 $F \cdot g^{-1}$ at constant current of 25 $mA \cdot g^{-1}$, but it decreases with the increase of the current. For comparison, activated carbon electrodes were tested also in Et_4NBF_4–PC electrolyte and a high initial specific capacitance of 24.4 $F \cdot g^{-1}$ was obtained, which means that the second electrolyte fits better to the specific porosity of the active carbonaceous material. The effect of charging potential on the cycling performances of the supercapacitors was also investigated. The control of energy flows in the power management system developed takes into account all important factors in order to obtain a flexible and adaptable power source.

Key words: nanostructured carbon, supercapacitors, biomaterials.

INTRODUCTION

Many research groups and companies work on the development of new more effective systems in order to respond to the enhanced needs of light and compact high capacity sources [1–6]. The most common electrical energy storage device is the battery, because it can store large amounts of energy in a relatively small volume and weight.

As it can be seen from Figure 1, the batteries**,** as well the fuel cells are very attractive from the point of view of energy density. But from the point of view of the power density, due to their complex electrochemical nature, they could not deliver the necessary current at a rate, sufficient for most of the power demanding applications. In the recent years new electrochemical energy-storage devices, such as supercapacitors are playing a crucial role in such applications, where they are coupled with batteries. The obtained hybrid power source effectively supplies energy for a long time and at the same time is capable of covering high power peaks both in consumption, and in charging. Such processes take place during acceleration and in energy recovery during braking of electrical vehicles [7–11].

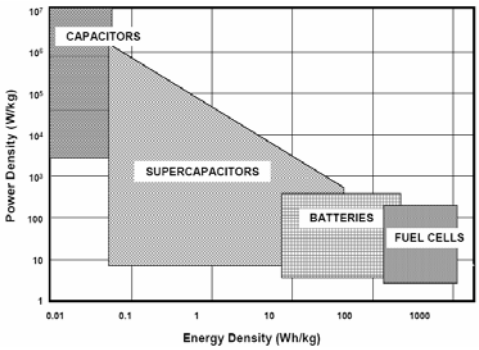

Fig. 1. Specification of various energy storage devices [6].

The study and modeling of the physical and electrochemical characteristics of nanoporous carbon are important for the development of electrical double layer capacitors. A very important problem is associated with the physical gas phase properties of a nanoporous material, like the nanopore diameter and pore size distribution, the conductivity and the accumulation of energy in the space-charge surface layer, i.e., the so-called capacitance of the thin layer determining the characteristic relaxation frequencies, specific energy and power densities and other characteristics of the supercapacitors. The chemical character of the carbon surface has a significant effect on its adsorptive properties. It is well known that ash-free carbons obtained in the presence of water vapour at high temperatures

* To whom all correspondence should be sent:
E-mail: mladen47@bas.bg

(above 800°C) possess a hydrophobic surface [12–15]. The surface becomes more hydrophilic, when it is covered with surface oxides formed after treatment with strong oxidants. The carbons, activated with water vapour or CO_2, possess alkaline character of the surface. Acidic oxygen groups on oxidized carbon surfaces produce cation exchange properties. Carbons activated with water vapour and CO_2 exhibit anion exchange capacity because basic surface oxides are always present, when carbons have been exposed to the atmosphere [16–18].

The aim of the present investigation is to obtain novel nanoporous carbon on the basis of biomaterial with different structure and chemical surface properties as well as preliminary electrochemical testing of the electrodes developed into supercapacitors with nonaqueous electrolyte.

EXPERIMENTAL

Preparation of nanoporous carbon with desired structure and chemical surface properties

200g of the mixture of tar from steam pyrolysis of apricot stones and furfural 50:50 are treated with H_2SO_4 (3%) at 160°C upon continuous stirring. The obtained solid product is heated to 600°C in a covered silica crucible with a heating rate of 10°C/min under nitrogen atmosphere. Steam activation with water vapour at 900°C for 1 h is used to obtain activated carbon with alkaline surface. The porous structure of carbon adsorbents is studied by using N_2 adsorption at 75K. The N_2 surface area and mesopores size distribution was determined using the BET equation and a procedure developed by Barret *et al*. [22] in which the apparent pore radius was calculated by the Kelvin equation [23]. The total pore volume (V_{total}) is derived from the amount of N_2 adsorbed at a relative pressure of 0.95, assuming that the pores are then filled up with liquid adsorbate. The Dubbin-Radushkevich equation was used to calculate the micropores volume (V_{micro}) [24]. The mesopores volume was calculated by subtracting V_{micro} from V_{total} i.e. ($V_{meso} = V_{total} – V_{micro}$).

Cell assembly and measurements

Sandwich-type symmetric cells were assembled in dry box. Three cells were produced denoted as: a) Cap-5 (carbon ACN-1, electrolyte 1 M $LiBF_4$–PC); b) Cap-7 (carbon ACN-1, electrolyte Et_4NBF_4–PC), c) Cap-9 (carbon Norit NK-1, electrolyte Et_4NBF_4–PC). The electrodes were prepared from a mixture of 90% activated carbon powder and 10% PTFE binder (Aldrich, 60% suspension in water) and pressed on Al discs (surface area 1.75 cm^2). The electrolytes (20 ppm H_2O) used in assembling two types of cells were 1 M $LiBF_4$–PC (propylene carbonate) and Et_4NBF_4–PC, (Aldrich p.a.) with a ceramic-mat separator. The electrodes were soaked in the electrolyte before cell assembling. The cell was enclosed in a metallic hermetically sealed can. The morphology of the activated carbon was examined by means of a scanning electron microscope JEOL-Superprobe 733 and T 200. The crystallographic structure of activated carbon ACN was identified by powder X-ray diffraction (XRD) with Cu Kα radiation using a Philips ARD 15 diffractometer. The BET surface area was measured with Area-METER, Stulien, Germany. Porosity analyses have been made on activated carbon powder with Autopore 9200 - Micromeritix.

The conductivities of the dry electrode and of the assembling cell were measured with C-R-L measurer – E7-8 at 1.5 kHz. Constant current charge-discharge cycling of the cell was carried out over voltages of 1.25–2.5 (2.7) V at current loading of 25, 50, 75 and 100 $mA \cdot g^{-1}$ with battery tester (IMK-10, BG) at room temperature. The data from the cycle tests of the laboratory cells were compared with the data of the commercial capacitor – Cap. Comers from Honeywell company, USA.

RESULTS AND DISCUSSION

Morphological and physical characterization

Fig. 2 shows the nanoporous structure of material ACN-1after heating of carbon at 750ºC.

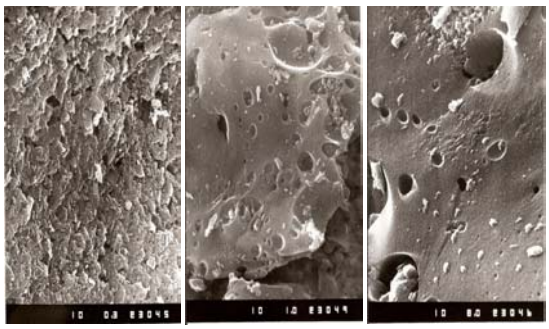

Fig. 2. SEM image of nanoporous carbon ACN-1.

In general, we assume that the activation results in an enlargement of existing small pores and oxidation of reactive site on the particles' surface.

N_2 (77K) adsorption isotherm of the obtained carbon is represented in Fig. 3. The N_2 isotherm character (a step increase with tendency for saturation) is indicative of its micro-porosity.

The adsorption investigations reveal that the activation with water vapour leads to the formation of microporous carbon. The surface area and volumes of micro-, meso- and macro- pores of carbon were measured, and they are shown in Table

1. The data show prevailing content of micropores in the obtained carbon. The micropore size distribution (Fig. 4) shows typical supermicroporosity (X_o = 1.3 nm).

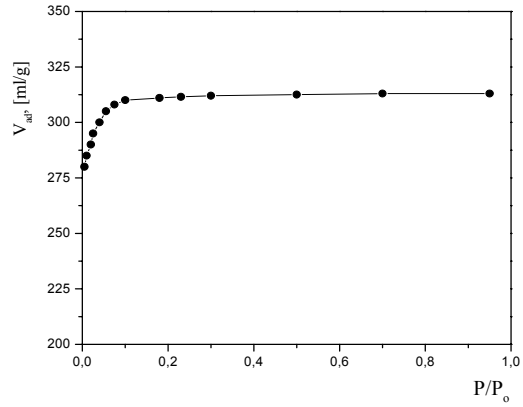

Fig. 3. N_2 (77 K) adsorption isotherm of nanoporous carbon ACN-1.

Differences in the pore size of the compared carbon materials could be observed in Fig. 4a, b. For sample ACN-1 the micro-pores prevail with average radius 1.25 nm, while for Norit NK-1 the average size is 0.7 nm.

The final product element composition of the activated carbon material is presented in Table 2.

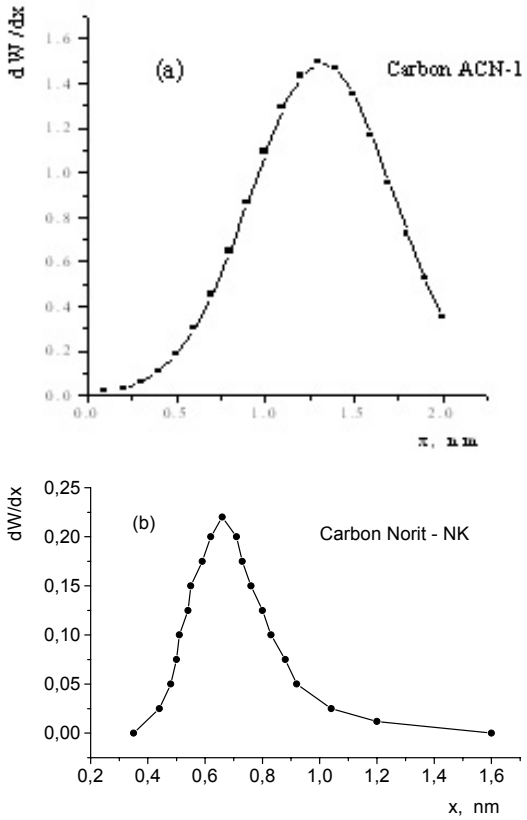

Fig. 4. Micropores size distribution of activated carbon ACN-1 from biomass products: (a) carbon ACN-1, (b) carbon Norit NK-1.

It could be seen from Table 1, that there is a difference between the values of the total volume of pores for the tested carbon materials. It is 0.717 $cm^3 \cdot g^{-1}$ for ACN-1 and 0.58 $cm^3 \cdot g^{-1}$ for Norit NK-1. The relative volume of ion-accumulating micropores in the newly synthesized carbon material is 0.43 $cm^3 \cdot g^{-1}$, while in the commercial probe this volume amounts to 0.280 $cm^3 \cdot g^{-1}$. The volume of mezzo-pores differs slightly for the both probes – correspondingly 0.130 and 0.150 $cm^3 \cdot g^{-1}$.

Fig. 5 represents the X-ray diffraction pattern for investigated material ACN-1.

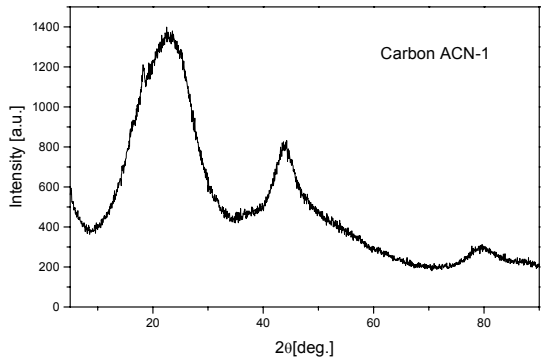

Fig. 5. XRD patterns of nanoporous carbon

X-ray diffraction pattern features three broad lines of carbon at 3.77 Å, 2.05 Å and 1.20 Å. The observed halo is typical for the amorphous materials. It confirms SEM's results about nanosised particles of the materials.

Table 1. Porosity characteristics of activated carbon obtained from mixture of biomass products.

Sample	S, $m^2 \cdot g^{-1}$	Pores volume, $cm^3 \cdot g^{-1}$			
		Total	Micro-	Meso-	Macro-
ACN-1	1050	0.717	0.430	0.130	0.157
Norit NK-1	600	0.58	0.280	0.150	0.180

Table 2. Elemental analysis of activated carbon (ACN-1) obtained from mixture of biomass products.

Sample	Proximate analysis, %			Elemental analysis, %				
	W	Ash	pH	C	H	N	S	O
ACN-1	5.1	0.76	7.0	81.14	2.56	0.28	0.54	15.48

The data in Table 2 show the low ash and sulphur contents, relatively high oxygen content and alkaline character of the carbon surface. For improving the quality of the obtained carbon, oxygen content has to be reduced.

Galvanostatic cycling

The symmetric capacitance cells were studied at constant current charge–discharge mode in the

voltage range 1.25–2.5V. The specific discharge capacitance of the electrodes was calculated from the data in accordance with the Eqn. (1):

$$C_f = 2I \frac{\Delta t}{m\Delta U}, \qquad (F \cdot g^{-1}) \qquad (1)$$

where I is current intensity, Δt – discharge time, ΔU – the voltage difference between the upper and lower potential limits and m - the mass of the carbon in one of the electrodes. The factor 2 reflects the fact that the total capacitance of the cell results from the capacities of the two equivalent single electrodes connected in series.

The voltage/time curves for two carbons ACN-1 and Norit NK-1 with different non-aqueous electrolytes are represented in Fig. 6a-c. Both charging and discharging times at this regime are changed slightly, which shows the stability of the capacity (16 $F \cdot g^{-1}$) through the cycling. The characteristics of the capacitor cell with Cap-5 construction, cycled at current 25, 50, 75 и 100 $mA \cdot g^{-1}$, at 25ºC are shown in Table 3. It can be seen that the specific capacity of the cell is decreased drastically. With the current increase to 100 $mA \cdot g^{-1}$, the cell utilizes only 14% of its nominal capacity. This behaviour could be caused by the electrolyte properties, as well as by the electrode mass low conductivity, which leads to high total resistance of the cell 1.2 mΩ.

In Figure 6b the charge-discharge curves of a cell Cap-7 are shown. They differ from the cell Cap-5 only by the electrolyte used, namely Et_4NBF_4 – PC. From the Figure 7 and Table 3 it could be seen that the cell Cap-7 24.4 $F \cdot g^{-1}$ (18 $F \cdot cm^{-3}$) shows about 40% more capacity compared with Cap-5. With the discharge current of 100 $mA \cdot g^{-1}$ it maintains more than 30% of its nominal capacity. This could be explained by the fact described in the work of Aurbach [10] that capacitors with nonaqueous electrolytes, having ions (cations) with smaller dimensions ($Et_4N^+ < Li^+$) could accumulate signify-cantly bigger capacity with respect to given carbon material, in this case – ACN-1.

In Figure 6c a typical charge-discharge depend-ency is shown of a sample Cap-9 on the basis of a commercial carbon Norit NK-1 with current charge 25 $mA \cdot g^{-1}$ utilizing electrolyte Et_4NBF_4–PC.

It can be seen from the figure that the profile of the dependency voltage–time for the sample Cap-9 is similar to that of the sample Cap-7 – carbon ACN-1. It should be mentioned that also for the commercial sample Cap-9 a good stability of the capacity with the cycling is observed, and that the capacity decreases by no more than 0.1% per cycle. It seems interesting to compare the data from testing the laboratory samples under higher current loads up to 100 $mA \cdot g^{-1}$ which are represented in Table 3.

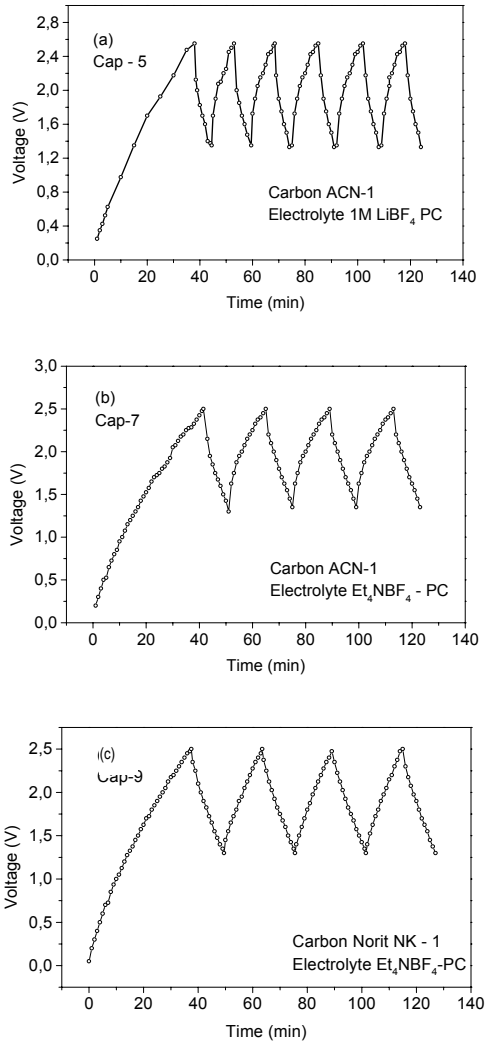

Fig. 6. Cycling performances of symmetric cells with nano-porous carbon electrodes in the voltage range of 1.25–2.5 V at current loading 25 $mA \cdot g^{-1}$: (a) cell with carbon ACN-1 and electrolyte 1 M $LiBF_4$– PC ; (b) cell with carbon ACN-1 and electrolyte 1 M Et_4NBF_4–PC, (c) cell with carbon Norit-NK_1 and electrolyte 1 M Et_4NBF_4–PC.

Table 3. Constant current charge/discharge data for supercapacitors type Cap-5, Cap-7 and Cap. Comers at window voltage 1.25–2.5 V.

No	Dis-charge current, $mA \cdot g^{-1}$	Specific capacity per electrode, $F \cdot g^{-1}$			
		Cap-5 (With cell capacity 0.6 F at load), 25 $mA \cdot g^{-1}$	Cap-7 (With cell capacity 1.0 F at load), 25 $mA \cdot g^{-1}$	Cap-9 (With cell capacity 1.16 F at load), 25 $mA \cdot g^{-1}$	Cap. Comers (With cell capacity 1.0 F at load), 25 $mA \cdot g^{-1}$
1	25	16.2	24.4	23.5	54
2	50	9.6	18.8	21.2	52
3	75	4.4	12.0	16.2	50
4	100	2.2	7.6	14.4	50

In Table 3 three types of cells are presented, which are different as carbon material, as well as the used electrolyte. These cells have total capacity approximately equal to the capacity of the comercial cell - Cap. Commers (Honeywell company) chosen for comparison.

It can be seen from the Table 3 that the capacity of the cell Cap-5 is falling down drastically with the load increase, and under the maximal load it is hardly 14% of C_f^o (C_f^o - nominal capacity). The cells Cap-7 and Cap-9 show practically equal capacity under slow discharge but at a load of 100 mA·g^{-1} the cell, built of carbon ACN-1, keeps 31% of its nominal capacity. The cell with the commercial material Norit NK-1 under the same regime preserves 61% of C_f^o. The most stable behaviour under high power loads was observed for the commercial capacitor (Cap-Commerce) where the loading slightly influences the discharge capacity whose value is 92% of the nominal capacity at 100 mA·g^{-1}.

The cause for such behaviour of ACN-1 despite the well developed pore structure and the appropriate pore size distribution (with prevailing micropores of 1–2 nm size) lies in the composition and the structure of the carbon. It has higher content of oxygen which, together with its structure, determines its lower conductivity, and is of substantial importance for its behaviour under higher power loads. Changes in the structure and composition of this carbon could be achieved through variations of the precursor content, and the conditions of its preparation.

Possible application in smart hybrid supercapacitor power system

In order to obtain better performance of electrochemical power sources, they should be considered as a system. All the decisive factors - the energy sources, the converters, and the overall exploitation conditions should be taken into account. The power flows need to be actively controlled, to assure the effectiveness of the energy system.

Figure 7 shows a typical electrical power management system. A load *M* (electric motor) is supplied by hybrid electric energy storage system (actively paralleled electrochemical battery *B* and supercapacitor bank *C*), and possibly generator *G* (dynamo, fuel-cell, wind generator, thermo-solar cell). This system structure presents a lot of possible applications: electric or hybrid vehicles, cranes, lifts, small electrically driven airplanes, local power systems and others. The connecting lines in the figure show the power flows between the system devices, visualizing their frequencies (by punctuations), and directions (by arrowheads).

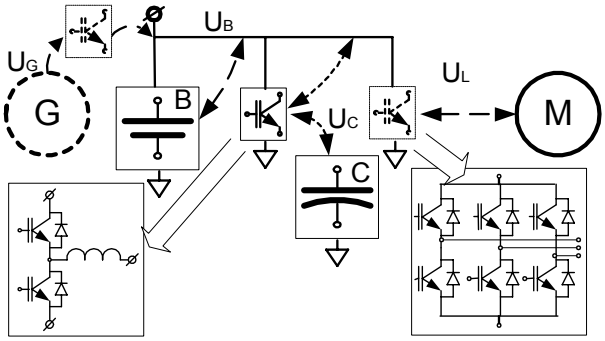

Fig. 7. Power management system with bi-directional converter.

In this case, there is only one DC to DC converter, which is a bi-directional, buck/boost converter [19]. This converter type allows changing the direction of the power flow, as well as stepping-down and stepping-up of the input/output voltages.

In the case of hybrid system consisting of supercapacitor and battery, or other combination of supercapacitor and electrochemical power source, there are several important interfaces, as shown in the figure. They determine at large the efficiency of the entire system: battery-supercapacitor, charging device-supercapacitor and battery, supercapacitor-load.

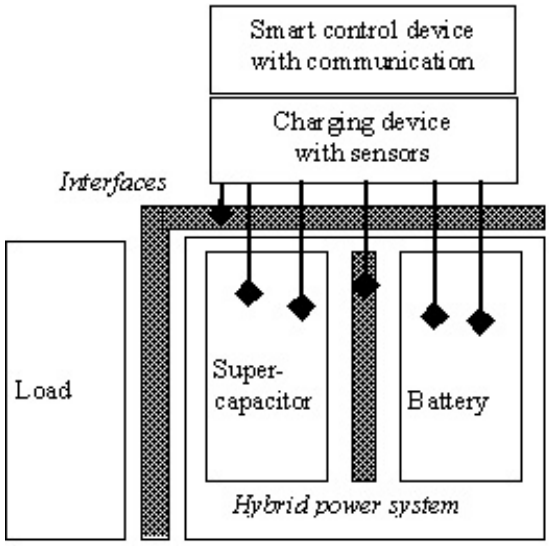

Fig. 8. Smart hybrid supercapacitor power system.

Energy flow through the interfaces should be observed and managed by the best possible expertise. The smart control device collects important information, such as number of cycles performed, current status of the supercapacitor and the battery, etc. This information is taken into account when negotiating the parameters of charge and discharge processes with the load or the charging device. The system is equipped with sensors for current, voltage, temperature, pressure measurement. It is not only a

simple data collecting device, but also actively controlling the processes of energy flow in correspondence with the goals set and the context recognized.

The smart control devices easily communicate and negotiate when assembled in larger networks, as in a windmill power plant, for instance. The purpose of the negotiation is to set the best parameters for the charge and discharge of each individual hybrid system with respect to its production technology, history of exploitation, current status. This could help in the process of achievement of much effective energy production and utilization.

CONCLUSION

The novel nanoporous furfural resin-derived carbon having improved pore size distribution, was synthesized by carbonization of a mixture of furfural and pyrolysed tar and steam activation. The BET surface area of carbon was 1140 $m^2 \cdot g^{-1}$. The EDL laboratory capacitor was built up with a total of 100 mg activated carbon. Electrochemical characteristics of the novel carbon material in two electrolytes: 1 M $LiBF_4$ and Et_4NBF_4 in PC solution were studied using cycling charge-discharge test at constant current.

It was shown that the furfural resin-derived carbon electrode material demonstrates very good capacitive characteristics. Although the specific gravimetric capacitance of the novel carbon in Et_4NBF_4 in PC solution (24 $F \cdot g^{-1}$) does not surpass that of the advanced activated carbon materials, however, the volumetric capacitance (over 18 $F \cdot cm^{-3}$) is excellent for non-aqueous supercapacitors, using the working voltage up to 2.5 V. The internal resistance of the laboratory supercapacitor was 1.2 mΩ and the stored capacitance was calculated to be 25 $mA \cdot g^{-1}$ at cell voltage 2.5 V.

The material properties, as well as the resulting system properties are taken into account when integrating the energy units into a power source. The power flows are actively controlled, to assure the energy system effectiveness.

***Acknowledgment**: This work is supported by the Bulgarian National Science Fund under contract TK-X-1705/12.2007*

REFERENCES:

1. J. Zhao, Ch. Lai, Y. Dai, J. Xie, *Mater. Lett.*, **61,** 4639 (2007).
2. C. Arbizzani, S. Beninati, M. Mastragostino, *J. Power Sources*, **174**, 648 (2007).
3. B.-J. Kim, S.-J. Park, *J. Colloid Interface Sci*., **315,** 791 (2007).
4. A. G. Pandolfo, A. F. Hollenkamp, *J. Power Sources*, **157**, 11 (2006).
5. M. Arulepp, J. Leis, M. Latt, F. Miller, K. Rumma, E. Lust, A. F. Burke, *J. Power Sources*, **162**, 1460 (2006).
6. M. Jayalakshmi, N. Venugopal, K. Phani Raja, M. M. Rao, *J. Power Sources*, **158,** 1538 (2006).
7. M. Bartsch, A. Braun, B. Schnyder, R. Kotz, O. Haas, *J. New Mater. Electrochem. Systems*, 2, 273 (1999).
8. J. Gamby, P. L. Taberna , P. Simon, J. F. Fauvargue, M. Chesneau, *J. Power Sources*, **101**, 109 (2001).
9. J. Zhao, Ch. Lai, Y. Dai, J. Xie, *Mater. Lett*., **61**, 4639 (2007).
10. G. Salitra, A. Soffer, L. Eliad, Y. Cohen, D. Aurbach, *J. Electrochem. Soc*., **147**, 2486 (2000).
11. A. Burke, *J. Power Sources*, **91**, 37 (2000).
12. N. Petrov, T. Budinova, M. Razvigorova, E. Ekinci, F. Yardim, V. Minkova, *Carbon*, **38**, 2069 (2000).
13. V. Minkova, M. Razvigorova, E. Bjornbom, R. Zanzi, T. Budinova, N. Petrov, *Fuel Process. Technol*., **70**, 53 (2001).
14. D. Savova, E. Apak, E. Ekinci, F. Yardim, N. Petrov, T. Budinova, M. Razvigorova, V. Minkova, *Biomass Bioenergy*, **21**, 133 (2001).
15. N. Petrov, T. Budinova, M. Razvigorova, J. Parra, P. Galiatsatou, *Biomass Bioenergy*, **32**, (2008) (in press).
16. F. Rodriguez-Reinoso, M Molina-Sabio, M. T. Gonzales, *Carbon*, **33**, 15 (1995).
17. M. T. Gonzales, F. Rodriguez-Reinoso, A. N. Garcia, A. Marcilla, *Carbon*, **35**, 159 (1997).
18. V. Minkova, S. P. Marinov, R. Zanzi, E. Bjornbom, T. Budinova, M. Stefanova, L. Lakov, *Fuel Process. Technol*., **62**, 45 (2000).
19. J. M. Miller, M. Prummer, A. Schneuwly, *Power Systems Design Europe*, **4**, 48 (2007).

СИНТЕЗ И ХАРАКТЕРИЗИРАНЕ НА НОВ НАНОСТРУКТУРИРАН ВЪГЛЕН ЗА СУПЕРКОНДЕНЗАТОРИ НА ОСНОВАТА НА БИОМАТЕРИАЛИ

М. Младенов[1], П. Златилова[1], Р. Райчев[1], С. Василев[1], Н. Петров[2], К. Белов[3], В. Тренев[3], Д. Ковачева[4]

[1] Институт по електрохимия и енергийни системи, Българска академия на науките, 1113 София
[2] Институт по органична химия, Българска академия на науките, 1113 София
[3] Централна лаборатория по мехатроника и приборостроене, Българска академия на науките, 1113 София
[4] Институт по обща и неорганична химия, Българска академия на науките, 1113 София

Постъпила на 23 юни 2007 г., Преработена на 2 юли 2008 г.

(Резюме)

Синтезиран е нанопорьозен въглероден материал чрез активиране с водна пара на предварително карбонизирана смес от фурфурол и пиролизиран катран от прасковени костилки. Полученият въглен е тестван като активен материал в суперкондензатор с неводен електролит, конструиран като двуелектродна клетка. Използвани са два типа неводни електролити в диапазон на работното напрежение 1.25–2.5V. Началният специфичен капацитет на клетката с електролит $LiBF_4$–PC е 16.2 $F \cdot g^{-1}$ при постоянна пътност на тока от 25 $mA \cdot g^{-1}$, който обаче намалява при повишаване на плътността на тока. За сравнение, активният материал беше тестван и с втори електролит Et_4NBF_4–PC и беше получен по-висок начален специфичен капацитет 24.4 $F \cdot g^{-1}$, което показва, че вторият електролит се съчетава по-добре със специфичната порьозност на активния въглероден материал. Изследвано е също и влиянието на потенциала при зареждане върху способността за циклиране на суперкондензаторите. Контролът на енергийните потоци в разработената система за управление на електрично захранване отчита всички важни фактори с оглед получаването на гъвкав и адаптивен енергиен източник.